

## Geometric Effect of Single or Double Metal-Tipped CdSe Nanorods on Photocatalytic H<sub>2</sub> Generation

Jung Up Bang,<sup>†,‡,||</sup> Seon Joo Lee,<sup>†,‡,||</sup> Jum Suk Jang,<sup>\*,§</sup> Wonyong Choi,<sup>§</sup> and Hyunjoon Song<sup>\*,†,‡</sup>

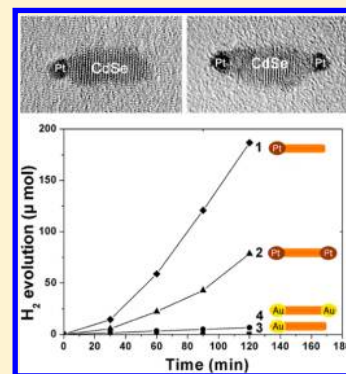
<sup>†</sup>Department of Chemistry, Korea Advanced Institute of Science and Technology, Daejeon, 305-701, Korea

<sup>‡</sup>Center for Nanomaterials and Chemical Reactions, Institute for Basic Science, Daejeon, 305-701, Korea

<sup>§</sup>School of Environmental Science and Engineering, Pohang University of Science and Technology, Pohang, 790-784, Korea

### S Supporting Information

**ABSTRACT:** In the present work, we focused on geometrical (single- or double-tipped) and compositional (Pt or Au) variations of active metal components in a well-defined CdSe nanorod system. These colloidal nanostructures were employed for photocatalytic hydrogen generation from water under the identical reaction conditions with visible light irradiation. The catalysts exhibited significant dependency of the catalytic activity, specifically on the catalyst geometry and the choice of the metal tips, determined by the energetic consideration of electron transfer to the metal tips and hole transfer to the sacrificial reagents on the CdSe nanorods.



**SECTION:** Energy Conversion and Storage; Energy and Charge Transport

Photocatalytic hydrogen generation is one of the potential reactions for the production of environmentally clean and renewable energy resources from sun light.<sup>1</sup> Although TiO<sub>2</sub> has been studied as a highly effective photocatalyst for decades, the wide bandgap of TiO<sub>2</sub> in the ultraviolet region shifted the research interest into semiconductors that absorb visible light, such as complex metal oxides,<sup>2</sup> nitrides,<sup>3</sup> and sulfides.<sup>4,5</sup> Among these materials, cadmium chalcogenides have mostly been used as essential elements in photocatalysts due to their narrow band gaps and band energies at relatively low potentials. Recently, several hybrid nanostructures of CdS and CdSe with metals have been synthesized and employed for the photosplitting of water.<sup>6,7</sup> In contrast to previous catalytic studies, the well-defined morphology and components of the hybrid nano-catalysts provided valuable information pertaining to the photoinduced charge separation and transfer processes during the reaction. Bao et al. explored photocatalytic hydrogen production using porous CdS nanostructures loaded with Pt nanoparticles in the presence of sacrificial reagents.<sup>8</sup> Banin et al. synthesized CdS nanorods decorated with noble metals and investigated the compositional effect on the photocatalytic activities.<sup>9</sup> Alivisatos et al. introduced CdSe seeds as a hole acceptor on Pt-tipped CdS rods, which facilitated photocatalytic stability as well as activity.<sup>10</sup> Although these systems were well characterized, each experiment was performed under distinct reaction conditions, and thus comparisons of different systems were not meaningful. In order to understand the factors that significantly affect the reaction activity, a reaction study using

various catalysts under identical experimental conditions is required.

In the present work, we focused on geometrical (single- or double-tipped) and compositional (Pt or Au) variations of active metal components on CdSe nanorods. These colloidal nanostructures were employed for photocatalytic hydrogen generation from water under identical reaction conditions with visible light irradiation ( $\lambda \geq 420$  nm). The catalysts exhibited significant dependency of the catalytic activity, both on the catalyst geometry and on the choice of the metal tips, as determined by the energetic consideration of hole transfer to the sacrificial reagents and electron transfer to the metal tips on the CdSe nanorods.

During the preparation of the catalyst, CdSe nanorods were synthesized in the presence of trioctylphosphine oxide and tetradecylphosphonic acid according to a method in the literature.<sup>11</sup> A mixture of the CdSe nanorods and Pt(II) acetylacetonate in 1,2-dichlorobenzene was injected into a hot solution of surfactants, specifically oleic acid, oleyl amine, and 1,2-hexadecanediol at 200 °C, and the reaction mixture was stirred for 4 min. After centrifugation, the particles were dispersed in toluene.

The addition of the Pt precursor (0.064 mmol) yielded single Pt-tipped CdSe nanorods (1). The transmission electron microscopy (TEM) image in Figure 1a shows that most of

**Received:** October 26, 2012

**Accepted:** December 5, 2012

**Published:** December 5, 2012

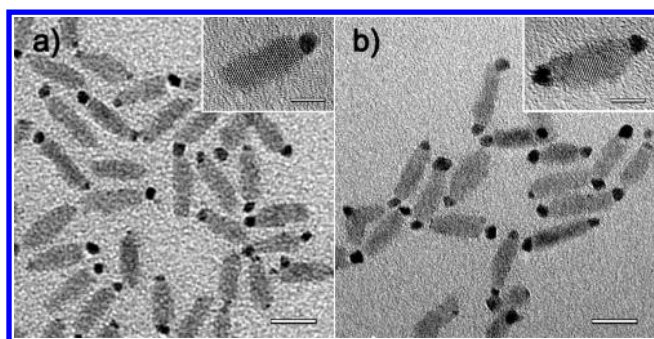


**Figure 1.** TEM images of (a) single (1) or (b) double (2) Pt-tipped CdSe nanorods. Insets are HRTEM images of single nanorods. The bars represent 10 nm for (a,b) and 5 nm for insets.

the CdSe nanorods have single Pt metal tips at the one end. A detailed analysis with more than 500 nanoparticles indicated that the product was 22% nontipped, 70% single Pt-tipped, and 7% double Pt-tipped CdSe nanorods (Figure S1a, Supporting Information). The CdSe nanorods are uniform with an average length of  $13.7 \pm 1.1$  nm and an average diameter of  $4.3 \pm 0.3$  nm, as estimated by counting 200 individual nanorods. An average size of the Pt dots on the CdSe nanorods was estimated to be  $1.3 \pm 0.2$  nm. A high-resolution TEM (HRTEM) image of a single nanorod shows that the CdSe nanorod is single-crystalline with a continuous lattice fringe pattern. The growth direction is along the  $\langle 001 \rangle$  axis, and the surface structure is smooth without any noticeable defects. A single Pt dot lies on the furthest-end, coming into direct contact with the rod surface.

A 2-fold increase in the amount of Pt precursor (0.13 mmol) yielded double Pt-tipped CdSe nanorods (2) on both sides. The TEM and HRTEM images show that the Pt particles are located at the two furthest ends of the individual CdSe nanorods (Figure 1b). The structural distribution of the product was 4% nontipped, 25% single Pt-tipped, and 71% double Pt-tipped CdSe nanorods (Figure S1b, Supporting Information). The average size of the Pt dots is  $1.2 \pm 0.3$  nm, nearly identical to that of 1. The X-ray diffraction (XRD) data of 1 and 2 have complex patterns, which correspond to a combination of the reflections of face-centered cubic Pt

(JCPDS No. 04–0802) and hexagonal wurzite CdSe (JCPDS No. 08–0459) (Figure S2, Supporting Information).

For comparison, single (3) and double (4) Au-tipped CdSe nanorods were synthesized using CdSe nanorods with dimensions identical to those of 1 and 2.<sup>12</sup> The average dimensions (length  $\times$  diameter) of the CdSe rods are  $(8.0 \pm 0.9) \times (4.3 \pm 0.3)$  nm (3) and  $(9.3 \pm 0.9) \times (4.3 \pm 0.4)$  nm (4), and the average diameters of the Au dots are  $5.1 \pm 0.6$  nm (3) and  $2.7 \pm 0.3$  nm (4), respectively (Figure S3, Supporting Information), according to an assessment of 200 nanoparticles. The XRD peaks confirm the face-centered cubic Au (JCPDS No. 04-0784) and wurzite CdSe (JCPDS No. 08-0459) (Figure S4, Supporting Information).

In the Pt-tipped CdSe nanorods, a low concentration of the Pt precursor led to the formation of single Pt tips, while the double-tipped structure was formed at a high Pt concentration. These observations indicated the formation of Pt tips by defect-mediated growth on the heterogeneous CdSe surface.<sup>13</sup> The furthest tip sites could be regarded as defects of the continuous single-crystalline CdSe, and the reduced Pt species were exclusively nucleated at such high-energy defect sites. These sites were isolated from each other, and thus the Pt dots grew to form single- or double-tipped structure upon a change in the Pt precursor concentration. In the Au-tipped CdSe nanorods, Au deposition also occurred at the defect sites, but the fast reduction rate of the Au precursor, AuCl<sub>3</sub>, could not uniformly form a single-tipped structure even under the low-concentration conditions. Instead, the single Au-tipped nanorods resulted after an increase in the precursor concentration due to a phenomenon similar to Ostwald ripening on a single nanorod.<sup>12</sup>

The optical properties of 1–4 were investigated using the corresponding colloidal dispersions in toluene. The UV–vis absorption of the CdSe nanorods shows the typical characteristics of excitonic band transitions, whereas the freestanding Pt nanoparticles show weak absorption levels (Figure 2a). The absorption spectra of 1 and 2 exhibit patterns analogous to that of the nanorods due to the tiny size (1.2 nm) of the Pt dots. 3 and 4 show very broad features with the tails extending to the low energy region in their spectra, reflecting the mixed electronic states of the metal and semiconductors.<sup>14</sup> On the other hand, the photoluminescence spectra of 1–4 exhibit the

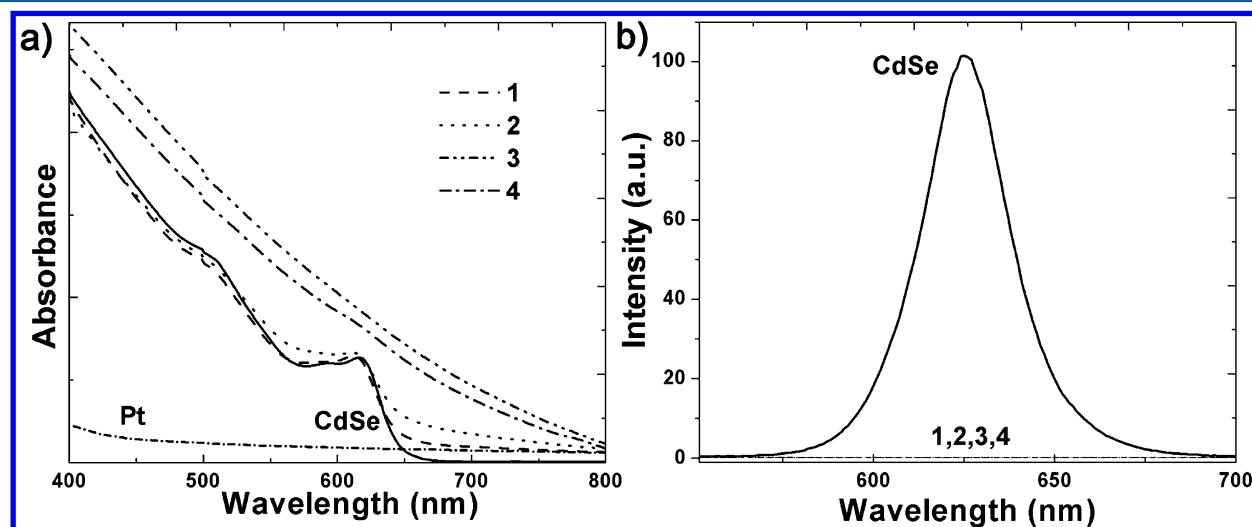


**Figure 2.** (a) UV–vis and (b) photoluminescence spectra of Pt nanoparticles, CdSe nanorods, and 1–4.

complete quenching of the emissions originating from the CdSe nanorods, regardless of the structure and the metal units (Figure 2b). This offers evidence that the junctions between the CdSe rods and the metal tips are electronically perfect, leading to effective electron transfer to the metals.<sup>15</sup>

The metal-tipped CdSe nanorods were employed as photocatalysts for hydrogen generation from water. Prior to the reaction studies, the nanorods were transferred from toluene to aqueous media via an exchange with mercaptoundecanoic acid. The resulting catalyst dispersions were stable for more than a few weeks in the cases of 1 and 2 (Figure S5, Supporting Information), but were relatively unstable to form particle aggregates in the cases of 3 and 4. The photocatalytic hydrogen generation reactions were performed under identical conditions.<sup>8</sup> The amounts of catalyst were standardized at 4.0 mg based on the CdSe unit. The reactions were carried out in a 0.35 M Na<sub>2</sub>SO<sub>3</sub>/0.25 M Na<sub>2</sub>S aqueous solution under visible light irradiation ( $\lambda \geq 420$  nm). Figure 3a exhibits the amount of H<sub>2</sub> evolution with time. After an induction period of 30 min for each catalyst, the rate of H<sub>2</sub> evolution reached a nearly constant value. The maximum rate of H<sub>2</sub> production is significantly dependent upon the choice of the catalysts in the order of 1 (145  $\mu\text{mol/h}$ ) > 2 (78  $\mu\text{mol/h}$ ) > 4 (3.3  $\mu\text{mol/h}$ ) > 3 (0  $\mu\text{mol/h}$ ). The apparent quantum yield of 1 was measured to be

0.63% at 454 nm. The catalyst stability of 1 was evaluated in a continuous 10 h reaction with intermittent N<sub>2</sub> purging every 2 h (Figure 3b). The induction period of the first run was observed for the activation of the catalyst, and the reaction activity maintained the maximum value for 10 h, which was consistent with or superior to those of other CdS/Pt nanostructured catalysts.<sup>6,8</sup>

In this catalytic system, visible light irradiation leads to the generation of electrons in the conduction band and holes in the valence band of the CdSe nanorod. The photogenerated electrons are quenched into the metal tips through the main exciton quenching pathway,<sup>9,16</sup> after which they are rapidly transferred to water, generating hydrogen molecules. The holes are moved to the surface of the nanorod and are then consumed by the sacrificial reagents of SO<sub>3</sub><sup>2-</sup> and S<sup>2-</sup> ions to form SO<sub>4</sub><sup>2-</sup> and S<sub>2</sub><sup>2-</sup>, respectively (Figure 4a and Figure S6, Supporting Information).<sup>5,9</sup> For the first run of the photo-reaction, similar induction periods were also reported in suspended CdSe nanocrystals due to the formation of Cd metal by light irradiation.<sup>17</sup>

It is known that Pt nanoparticles are the best proton reduction cocatalyst for photocatalysis. On the other hand, the electron flow from Au dots to a solvent is rather slow. As a result, a substantial amount of charge accumulates on the Au dots, and equilibration of the Fermi energy occurs between the CdSe and the metal. These phenomena were investigated in detail in ZnO–noble metal hybrid materials.<sup>18</sup> The poor dispersion, particularly of 3 in the reaction media, is another reason for the results showing nearly zero activity.

Unexpectedly, the activity of the single-tipped 1 was found to be better than that of the double-tipped 2, although the Pt loading of 1 was only half of the Pt amount of 2. The actual elemental analysis of the reaction mixtures containing the catalysts was carried out using inductively coupled plasma-atomic emission spectroscopy (ICP-AES). The data pertaining to the reaction mixture containing 1 (Cd: 695 ppm; Se: 467 ppm; Pt: 109 ppm) confirms the existence of half of the Pt concentration of 2 (Cd: 630 ppm; Se: 454 ppm; Pt: 252 ppm). The average Pt particle size is nearly identical in both structures. Consequently, it is reasonable to assume that such a difference in the reactivity is mainly attributable to the geometrical effect of the Pt tips on the CdSe nanorods. To investigate photoelectrochemical characteristics, 1 and 2 were drop-casted onto SnO<sub>2</sub>/ITO electrodes, and the photocurrents were measured under visible light illumination ( $\lambda \geq 420$  nm) in the presence of sacrificial reagents in an aqueous solution. Linear sweep voltammograms showed that significant photocurrents were generated by light illumination with the negligible dark currents (Figure 4b).<sup>16</sup> The photocurrent density of 1 was measured to be 0.20 mAcm<sup>-2</sup> at -0.2 V vs Ag/AgCl, which is three times larger than that of 2 (0.07 mAcm<sup>-2</sup>). The photocurrent density of the CdSe nanorods is 10 times lower than that of 1, indicative of the role of the Pt tips as an electron transfer mediator (Figure S7, Supporting Information).

The large photocurrent generation in 1 indicates that a unidirectional arrangement of metal and semiconductor domains is essential for photoinduced charge separation and transfer to the reagents. The effect of single-tipped structure on charge separation, which is superior to that of double-tipped type, needs to be explored by further studies. For the issue of charge transfer to the reagent, the tip regions are commonly regarded as highly active areas, and the sacrificial reagents,

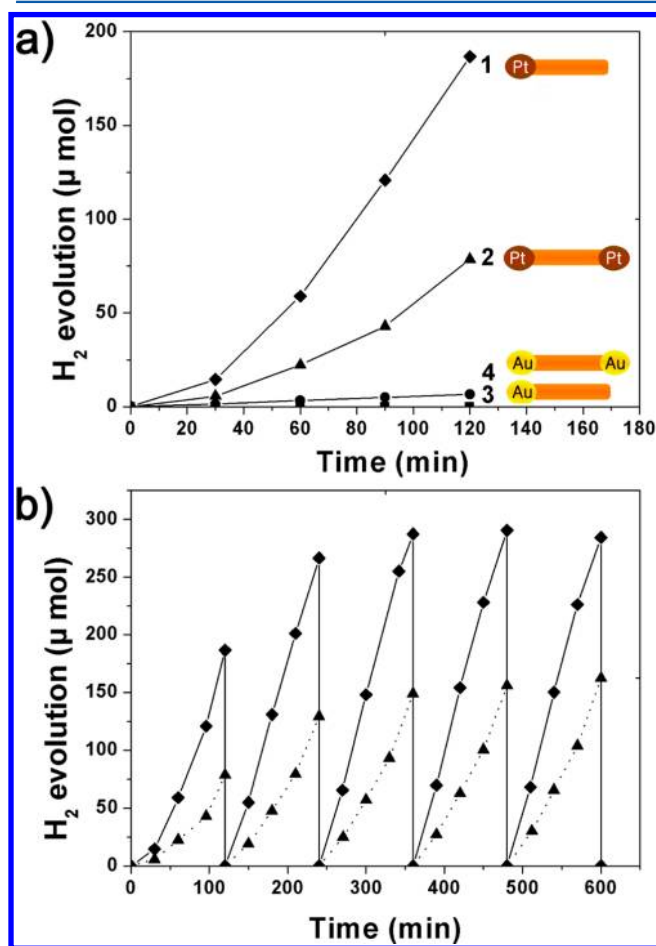


**Figure 3.** (a) Time course of H<sub>2</sub> evolution by 1 (◆), 2 (▲), 3 (■), and 4 (●); 4.0 mg catalysts based on the CdSe amount in a 0.35 M Na<sub>2</sub>SO<sub>3</sub>/0.25 M Na<sub>2</sub>S aqueous solution;  $\lambda \geq 420$  nm. (b) Time course of H<sub>2</sub> evolution by 1 (◆) and 2 (▲). The reaction was carried out for 10 h with intermittent N<sub>2</sub> purging every 2 h.



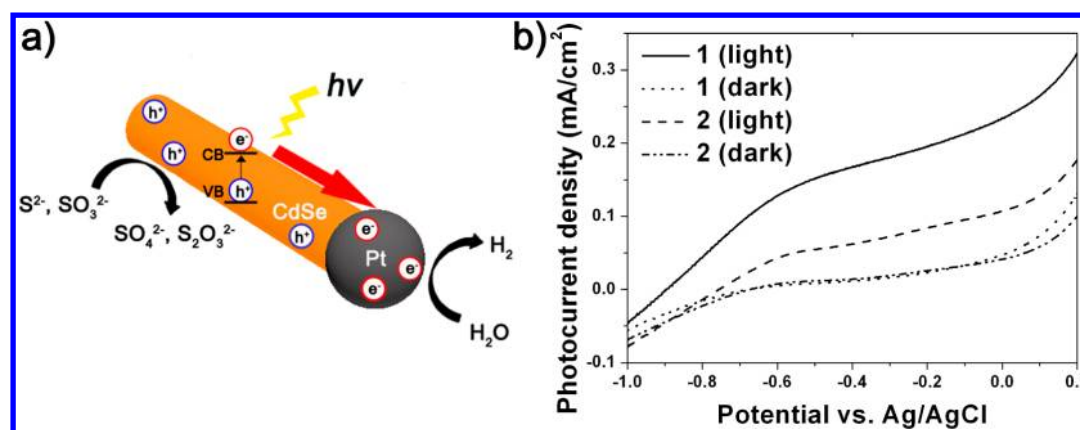


**Figure 4.** (a) Schematic representation of photocatalytic H<sub>2</sub> generation on 1. (b) Linear sweep voltammograms of the catalysts at a scan rate of 10 mVs<sup>-1</sup> under light irradiation ( $\lambda \geq 420$  nm).

SO<sub>3</sub><sup>2-</sup> and S<sup>2-</sup> ions, are likely to receive the holes through these sites.<sup>8</sup> The single Pt-tipped structure has the tip of a CdSe nanorod directly open to the reagent, where the hole transfer favorably occurs. However, in the double Pt-tipped structure, both tips are already occupied by Pt dots. Therefore, the holes must be transferred to the reagents through the less active walls having no defects with strong coordination of the surfactants.

In conclusion, the geometry of the catalyst structure is very important to facilitate the photoinduced catalytic generation of hydrogen. The single Pt-tipped CdSe nanorods produced ~50% more hydrogen than the double Pt-tipped structure, although the Pt loading of the former was only half that of the latter. These findings imply that the rational design of photocatalysts with a well-defined geometry and feasible compositions would maximize the photoconversion efficiency in desired reaction pathways.

## ■ ASSOCIATED CONTENT

### Supporting Information

Experimental details, TEM images, XRD data, and linear sweep voltammograms of metal-tipped CdSe nanorods. This material is available free of charge via the Internet at <http://pubs.acs.org>.

## ■ AUTHOR INFORMATION

### Corresponding Author

\*E-mail: [hsong@kaist.ac.kr](mailto:hsong@kaist.ac.kr) (H.S.); [jangjs75@postech.ac.kr](mailto:jangjs75@postech.ac.kr) (J.S.J.).

### Author Contributions

†These authors contributed equally.

### Notes

The authors declare no competing financial interest.

## ■ ACKNOWLEDGMENTS

This work was supported by the Research Center Program of IBS (Institute for Basic Science) in Korea. This work was also supported by the National Research Foundation of Korea (NRF) grant funded by the Korea Government (MEST) (2012-005624) and by the MKE (The Ministry of Knowledge Economy), Korea, under the ITRC support program (NIPA-2012-H0301-12-1009).

## ■ REFERENCES

(1) Osterloh, F. E. Inorganic Materials as Catalysts for Photochemical Splitting of Water. *Chem. Mater.* **2008**, *20*, 35–54.

(2) Kudo, A.; Omori, K.; Kato, H. A Novel Aqueous Process for Preparation of Crystal Form-Controlled and Highly Crystalline BiVO<sub>4</sub> Powder from Layered Vanadates at Room Temperature and Its Photocatalytic and Photophysical Properties. *J. Am. Chem. Soc.* **1999**, *121*, 11459–11467.

(3) Maeda, K.; Takata, T.; Hara, M.; Saito, N.; Inoue, Y.; Kobayashi, H.; Domen, K. GaN:ZnO Solid Solution as a Photocatalyst for Visible-Light-Driven Overall Water Splitting. *J. Am. Chem. Soc.* **2005**, *127*, 8286–8287.

(4) Tsuji, I.; Kato, H.; Kobayashi, H.; Kudo, A. Photocatalytic H<sub>2</sub> Evolution Reaction from Aqueous Solutions over Band Structure-Controlled (AgIn)<sub>x</sub>Zn<sub>2(1-x)</sub>S<sub>2</sub> Solid Solution Photocatalysts with Visible-Light Response and Their Surface Nanostructures. *J. Am. Chem. Soc.* **2004**, *126*, 13406–13413.

(5) Jang, J. S.; Yu, C.; Choi, S. H.; Ji, S. M.; Kim, E. S.; Lee, J. S. Topotactic Synthesis of Mesoporous ZnS and ZnO Nanoplates and Their Photocatalytic Activity. *J. Catal.* **2008**, *254*, 144–155.

(6) Frame, F. A.; Osterloh, F. E. CdSe-MoS<sub>2</sub>: A Quantum Size-Confined Photocatalyst for Hydrogen Evolution from Water under Visible Light. *J. Phys. Chem. C* **2010**, *114*, 10628–10633.

(7) Berr, M.; Vaneski, A.; Susha, A. S.; Rodríguez-Ferbández, J.; Döblinger, M.; Jäckel, F.; Rogach, A. L.; Feldmann, J. Colloidal CdS Nanorods Decorated with Subnanometer Sized Pt Clusters for Photocatalytic Hydrogen Generation. *Appl. Phys. Lett.* **2010**, *97*, 093108.

(8) Bao, N.; Shen, L.; Takata, T.; Domen, K. Self-Templated Synthesis of Nanoporous CdS Nanostructures for Highly Efficient Photocatalytic Hydrogen Production under Visible Light. *Chem. Mater.* **2008**, *20*, 110–117.

(9) Elmalem, E.; Saunders, A. E.; Costi, R.; Salant, A.; Banin, U. Growth of Photocatalytic CdSe–Pt Nanorods and Nanonets. *Adv. Mater.* **2008**, *20*, 4312–4317.

(10) Amirav, L.; Alivisatos, A. P. Photocatalytic Hydrogen Production with Tunable Nanorod Heterostructures. *J. Phys. Chem. Lett.* **2010**, *1*, 1051–1054.

(11) Peng, Z. A.; Peng, X. Nearly Monodisperse and Shape-Controlled CdSe Nanocrystals via Alternative Routes: Nucleation and Growth. *J. Am. Chem. Soc.* **2002**, *124*, 3343–3353.

(12) Mokari, T.; Sztrum, C. G.; Salant, A.; Rabani, E.; Banin, U. Formation of Asymmetric One-Sided Metal-Tipped Semiconductor Nanocrystal Dots and Rods. *Nat. Mater.* **2005**, *4*, 855–863.

(13) Habas, S. E.; Yang, P.; Mokari, T. Selective Growth of Metal and Binary Metal Tips on CdS Nanorods. *J. Am. Chem. Soc.* **2008**, *130*, 3294–3295.

(14) Shaviv, E.; Schubert, O.; Alves-Santos, M.; Goldoni, G.; Felice, R. D.; Vallée, F.; Fatti, N. D.; Banin, U.; Sönnichsen, C. Absorption Properties of Metal–Semiconductor Hybrid Nanoparticles. *ACS Nano* **2011**, *5*, 4712–4719.

(15) Mokari, T.; Rothenberg, E.; Popov, I.; Costi, R.; Banin, U. Selective Growth of Metal Tips onto Semiconductor Quantum Rods and Tetrapods. *Science* **2004**, *304*, 1787–1790.

(16) Kim, H.; Kim, J.; Kim, W.; Choi, W. Enhanced Photocatalytic and Photoelectrochemical Activity in the Ternary Hybrid of CdS/TiO<sub>2</sub>/WO<sub>3</sub> through the Cascadal Electron Transfer. *J. Phys. Chem. C* **2011**, *115*, 9797–9805.

(17) Holmes, M. A.; Townsend, T. K.; Osterloh, F. E. Quantum Confinement Cntrolled Photocatalytic Water Aplitting by Suspended CdSe Nanocrystals. *Chem. Commun.* **2012**, *48*, 371–373.

(18) Wood, A.; Giersig, M.; Mulvaney, P. Fermi Level Equilibration in Quantum Dot–Metal Nanojunctions. *J. Phys. Chem. B* **2001**, *105*, 8810–8815.